

# MODELING OF PHYSICAL PROPERTIES OF METAL FOAM FOR INDUSTRIAL HEAT EXCHANGER

**\*Thokre Manisha Rajkumar, \*\*Dr. Kakasaheb Chandrakant Mohite**

*\*Research Scholar, \*\*Research Supervisor,  
Department of Physics,  
Arunodaya University,  
Itanagar, Arunachal Pradesh*

---

## ABSTRACT

*Due to their high heat conductivity and robust physical properties, metals are commonly used in the creation of temperature exchangers. Metals such as copper, aluminum, and stainless steel will see the most use. While both aluminum and copper have high thermal conductivity, they also have high thermal expansion coefficients. The thermal conductivities of materials with low CTEs, such as copper/tungsten and copper/molybdenum, are often lower than that of aluminum. In order to quantify the metal foam's improved heat transmission, studies were conducted on both metal foam and hollow channel. Different rates of cooling air flow were used to measure the surface temperatures. The surface temperature of metal foam was found to be far lower than previously thought.*

**Keywords:** *Physical properties, heat transfer, exchanger, metal, temperature*

## INTRODUCTION

Metal foams have emerged as a fascinating class of materials with unique properties that have garnered significant attention in recent years. These foams are characterized by a high porosity structure consisting of interconnected metal cells or pores, resulting in a lightweight material with exceptional mechanical, thermal, and acoustic properties. The ability to tailor these properties makes metal foams highly desirable for a wide range of applications, particularly in the field of heat exchangers.

Heat exchangers play a crucial role in various industrial processes, including power generation, chemical processing, refrigeration, and HVAC systems. The primary function of a heat exchanger is to transfer thermal energy between two fluids while maintaining their separation. Traditionally, heat exchangers have been constructed using solid materials such as metals or alloys. However, these conventional designs often suffer from limitations such as high weight, increased pressure drop, and reduced heat transfer efficiency.

The unique structure of metal foams offers the potential to overcome these limitations and improve the performance of heat exchangers. The high porosity of metal foams provides a large surface area for heat transfer, while their low density results in reduced weight. Additionally, the interconnected

pore structure allows for enhanced fluid mixing, promoting convective heat transfer. Moreover, metal foams exhibit excellent thermal conductivity, making them highly efficient for heat exchange applications.

The successful utilization of metal foams in heat exchangers relies on a comprehensive understanding of their physical properties and behavior. These properties include thermal conductivity, pressure drop, and heat transfer performance, which directly influence the overall efficiency of a heat exchanger. Therefore, it is essential to develop mathematical models that accurately predict these properties and enable the optimization of metal foam-based heat exchanger designs.

## LITERATURE REVIEW

Helically coiled tubes are being used in a range of applications incorporating food. Nuclear reactor processing, miniature heat exchangers and heat restoration devices, medical apparatus, and chemical processing. In comparison to straight tubes, helical coils are more practical due to their small size and high heat transfer coefficients. By inducing centrifugal forces to operate on the moving liquid, the coils' curvature will increase the heat transfer coefficients and lead to the promotion of more flow.

Liquid that has been sucked from the inside of the tube travels down the conduit's center toward the outside divider, and then returns to the internal structure via the outlet section. Specifically in laminar flow, heat transmission and temperature are boosted by the second flow. However, in contrast to straight pipework, the amount of effort that is required to tilt a given mass quickly increases. The combination of these factors increased the cost of heat transmission and made temperatures more consistent, both of which might be advantageous in the processing of food.

Although helical coils' benefits in vertical pipe heat exchangers have been thoroughly investigated and heat transfer equations have been developed, there is still room for improvement. Such studies are typically limited in scope to either consistently high wall temperatures or steady wall fluxes.

While there are many studies available on the outdoors heat transfer coefficients, these only account for a standard wall temperature range and a standard wall heat flux from the coil, and so far no comprehensive study has been conducted on the state by a fluid as the heat transfer moderate on the exterior of the coil. In this study, the materials used control a helical heat exchanger between fluids, where steady-state conditions for either the wall temperature or the wall heat flux are out of the question.

When applied to alloys after engineering operations, the maker recommends standard stacking among the innovative CoCrMo alloy analog. All ceramics designed to work with a cold temperature expansion (CTE) ratio of  $15.2 \times 10^6/K$  can be used, as this is the ratio of the cold weather growth of the new alloy. The strength of the metal-ceramic system is determined by the strength of the connection between the metal and ceramic, which must be able to withstand the forces present in the tooth cavity.

Depending on the nature of the damage, a combination of ceramic platform and veneering may be crucial in determining the overall technical strength of the repair. To fuse the ceramic to the metal, just a little amount of CTE mismatch pressure is required. The metal-ceramic connection relies on a combination of chemical, mechanical, and van der Waals forces. Oxides formed during burning form a chemical link between ingredients, forming metallic, ionic, and covalent bonds in the ceramic. Roughness of the mixture surface and, by extension, van der Waals forces, often play a decisive role in determining the strength of the mechanical connection.

Ceramic FDPs are known for their longevity, but this can only be achieved by creating a strong link between the opaque component and the metal. Chemisorptions cause the metal-ceramic link by affecting the surface oxides of the ceramic and their resulting chemical reaction. During the ceramic's wetting process and subsequent burning, these oxides will form.

Extensive analysis has shown that an increase in the oxide covering's breadth can significantly weaken the sheet metal-ceramic binding strength in base alloys. According to this study, Girobond NB, a solid alloy, had the thickest oxide coatings on its surface, whereas Ceramill Sintron, a cheaper metal, had the thinnest. The oxide surface stratum established with the layering process may account for the pattern seen in Girobond NB specimens, which showed behaviors in lower ideals than Ceramill Sintron. The Designing ceramic's initial practical use led to the discovery of an important influence of alloy type on bond strength.

## EXPERIMENTAL SETUP

A heat exchanger test setup has been developed to put thermally sprayed metal foam through its paces at high temperatures. The performance of a Ni foam heat exchanger was measured using the test apparatus seen in Fig. 1, which was modeled in SOLIDWORKS. The following are the four components of the testing apparatus.

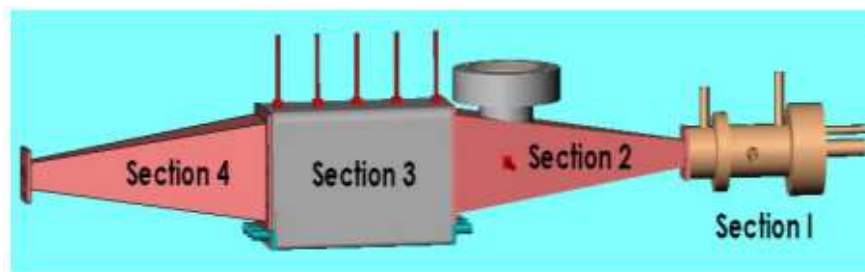


**Figure 1: Heat Transfer Test Rig**

### Section 1

The combustion chamber is made of copper and measures 20mm across on the interior. Internal design pressure is limited to no more than 2.0 MPa. According to ASME standards, the combustor tube has a wall thickness of 4mm. Water is utilized in the cooling jacket that surrounds the combustion

chamber. A premixed injector is used to facilitate the union of fuel and air. The injector is constructed of brass instead of a softer metal like copper since it is more challenging to drill small diameter holes in.

## **Section 2**

Stainless steel was used to create the igniter. It has a thickness of 4 mm and a length of 255 mm. portion III, the testing portion, is linked to the combustion chamber through this passageway. This duct has a dual purpose: it redirects exhaust from the combustion chamber to the test section, which has a much larger input diameter (80 mm) than the chamber's exit (15 mm). It has a built-in igniting mechanism with a crystal pane for seeing the sparking action.

## **Section 3**

A metal channel with an 80mm x 80mm cross section serves as the Test Section. Walls of the channel measure 4mm in thickness and 250mm in length and are constructed of stainless steel. It is a section of the examination. Ni foam heat exchangers or hollow metal channels are used for the bottom wall.

## **Section 4**

The purpose of the convergent section in gas temperature measurement At the end of the testing area is a convergent portion that is 250mm in length. This is the vent for the released gases.

## **EXPERIMENTAL PROCEDURE**

At first, two mass flow meters regulate and measure the CH<sub>4</sub> and compressed air flows for the test's stabilized combustion in a premixed methane-air burner. The igniting procedure within the diverging section may be observed through the crystal glass. Water is used to cool the combustion chamber, which has its own intake and output pipes. Mass flow controllers are installed at the Ni foam heat exchanger's intake and output to regulate the flow of cooling air. The temperature may be adjusted by adding nitrogen through the combustor's side vents. Five locations in the test section are equipped with K-type thermocouples for monitoring the exhaust gas temperature and the top surface temperature of the Ni foam heat exchanger/hollow channel. The Alumina double bore tubes act as a shield for the thermocouples. Pressure fittings are used to secure these tubes to the top of the test section. AREMCO's thermally conductive paste (597-A pyroDuct) is used to adhere the thermocouples to the heat exchanger's surface. The temperature of the air entering and leaving the Ni foam heat exchanger is measured by two thermocouples. In order to verify that the ignition has been turned on, one thermocouple is placed on the ignitor itself.

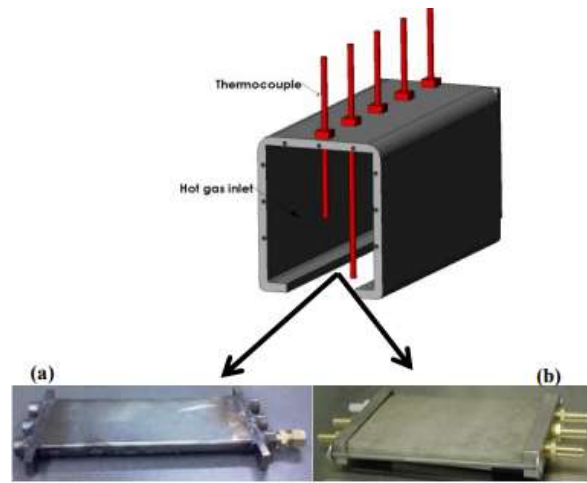


**Figure 2: The bottom of section 3 is replaced with (a) hollow channel (real image) (b) metal foam for performing different experiments (real image)**

### **The Hollow Channel**

In the first experiment, a hollow stainless steel metal box (70mm x 210mm x 10mm in thickness) was used as a reference point against which the performance of the metal foam heat exchanger could be evaluated. This duct is used to circulate room-temperature air at velocities ranging from 20 to 60 SLPM. Once the system has reached a steady state, the surface temperature is measured.

### **Ni Foam Heat Exchanger**

To make the heat exchanger, a rectangular piece of Ni foam is cut to dimensions of 70 mm by 200 mm. At CACT, they've come up with a novel way to deposit Inconel 625 skins over metal foam. First, a paste made from resin and metal powder is used to fill the metal foam's pores. Five hours of heat treatment at varying temperatures are then applied to the sample. The points or struts of the metal foam are revealed after heat treating the sample and grit blasting it at low pressure. The coating thickness of 300 microns is achieved by spraying the sample using a wire arc spraying method, which is the final stage in the manufacturing procedure. In order to remove the metal particles, the thermally sprayed sample is burnt at a high temperature, gasifying the resin.

During the experiment, the flow rate of the cooling air via the metal foam heat exchanger is varied. Once the system has reached a steady state, temperature readings are taken. Real photos of metal foam before and after thermal spray coating are shown in Fig. 3.



**Figure 3: Real images of (a) Metal foam (b) Metal foam heat exchanger after thermal spray coating**

**RESULTS**

Heat exchanger performance may be evaluated by solving the appropriate equations. Our simulation was compared to the performance of a heat exchanger with a parallel flow configuration. Flow configuration is shown in Fig. 5. As can be observed in Fig. 4, both the hot and cold gases enter the heat exchanger from one side and leave from the other. Neither a constant wall temperature nor a constant wall heat flow characterizes the heat transfer issue at hand. The rate of heat transfer between the hot and cold parts of a heat exchanger may be expressed using a straightforward mathematical correlation as follows:

$$\dot{Q} = UA_S \Delta T_{lm} \tag{1}$$

where  $A_S$  is the area of heat exchange between the hot and cold zones, and  $U$  is the average coefficient of thermal expansion. and  $\Delta T_{lm}$  is the logarithmic mean temperature defined as:

$$\Delta T_{lm} = \frac{\Delta T_1 - \Delta T_2}{\ln(\Delta T_1 / \Delta T_2)} \tag{2}$$

where  $\Delta T_1$  and  $\Delta T_2$  are the fluid input and fluid discharge temperatures, respectively.

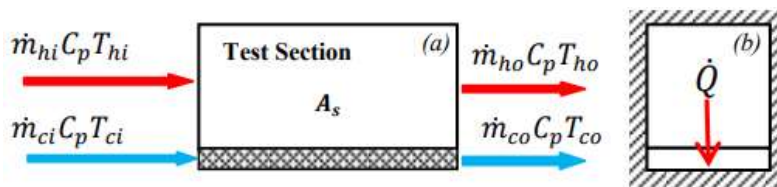


**Figure 4: Heat balance on test section (a) Side view (b) Cross section view**

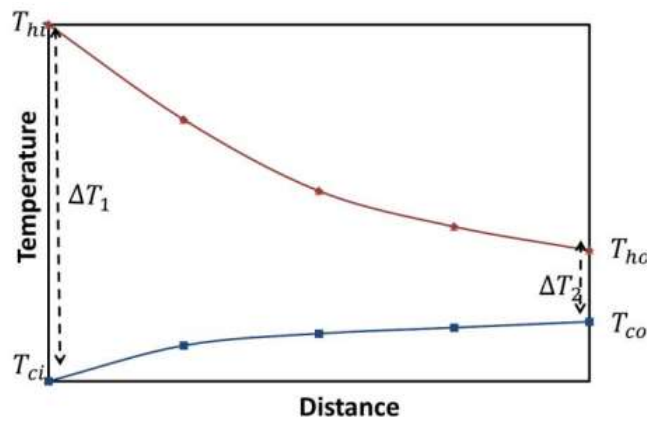


**Figure 5: Schematic of parallel flow heat exchanger**

The resistance analysis may be used to make an approximation of the heat transfer coefficient of the cold section  $h_c$  under the boundary condition. Since the boundary condition is neither a constant heat flow nor a constant surface temperature, the hot section heat transfer coefficient cannot be determined using the traditional analytical methods. Therefore, the heat transfer coefficient should be calculated using a treatment of varying surface temperatures.

For various airflow rates, the surface temperature of the hollow channel is depicted in Fig. 6 along the length of the channel. Increasing the pace at which cooling air is fed through the hollow channel results in a decreasing temperature profile throughout the distance, as shown in the figure.

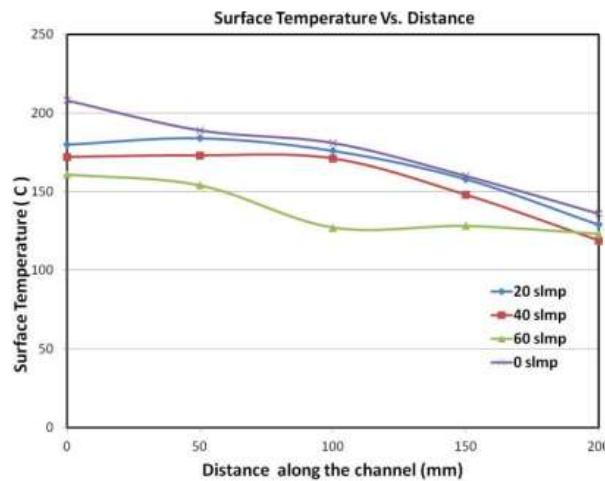


**Figure 6: Surface temperature vs. distance along the test section for hollow channel for different cooling flow rates**

Surface temperatures of metal foam and hollow channel are shown in Fig. 7. Different rates of cooling air flow (i.e., 20 slmp, 40 slmp, and 60 slmp) are used to calculate average surface temperatures. The



average surface temperature drops in both scenarios, as seen in the image. When using metal foam, there is a noticeable drop in surface temperature.

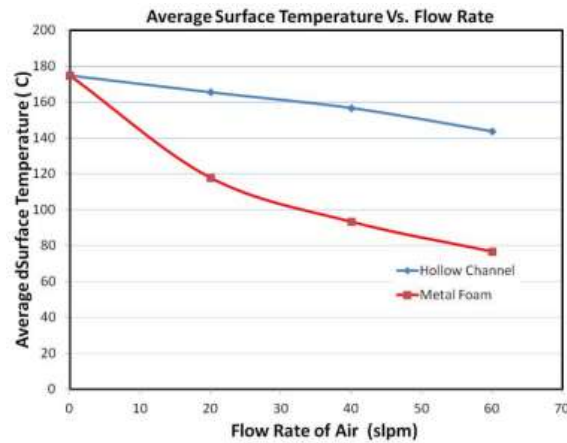


**Figure 7: Average Surface temperature of metal foam and Hollow channel**

## CONCLUSION

Incorporating the data by tubes and sheets for circulation management and heat transmission may be necessary for effective usage of metallic foam materials in heat exchange devices. Pipes and other solid materials have been studied for their potential in the development of advanced, multifunctional heat exchange equipment for a variety of customers. The quality of the connection between the foam and the stable material through which heat is transferred is a major consideration in the design of complicated heat exchangers.

## REFERENCES: -

- [1] Huisseune, Henk, et al. "Comparison of metal foam heat exchangers to a finned heat exchanger for low Reynolds number applications." *International Journal of Heat and Mass Transfer* 89 (2015): 1-9.
- [2] Alvandifar, N., M. Saffar-Avval, and E. Amani. "Partially metal foam wrapped tube bundle as a novel generation of air cooled heat exchangers." *International Journal of Heat and Mass Transfer* 118 (2018): 171-181.
- [3] Lu, Wei, et al. "Analytical solutions of force convective heat transfer in plate heat exchangers partially filled with metal foams." *International Journal of Heat and Mass Transfer* 110 (2017): 476-481.
- [4] Liu, Gang, Blair R. Tuttle, and Sarit Dhar. "Silicon carbide: A unique platform for metal-oxide-semiconductor physics." *Applied Physics Reviews* 2.2 (2015): 021307.



- [5] Hsiao, Yu-Che, et al. "Fundamental physics behind high-efficiency organo-metal halide perovskite solar cells." *Journal of Materials Chemistry A* 3.30 (2015): 15372-15385.
- [6] Morsali, Seyedreza, et al. "Multi-physics simulation of metal printing at micro/nanoscale using meniscus-confined electrodeposition: Effect of environmental humidity." *Journal of Applied Physics* 121.2 (2017): 024903.
- [7] Chen, Zhiquan, et al. "Multiple plasmon-induced transparency effects in a multimode-cavity-coupled metal–dielectric–metal waveguide." *Applied Physics Express* 10.9 (2017): 092201.
- [8] Yang, L. F., et al. "Prediction of spin-dependent electronic structure in 3 d-transition-metal doped antimonene." *Applied Physics Letters* 109.2 (2016): 022103.
- [9] Wu, Haoyu, et al. "Nanoscale heat transfer in the head-disk interface for heat assisted magnetic recording." *Applied Physics Letters* 108.9 (2016): 093106.
- [10] Ito, Kota, et al. "Parallel-plate submicron gap formed by micromachined low-density pillars for near-field radiative heat transfer." *Applied Physics Letters* 106.8 (2015): 083504.
- [11] Ijiro, T., and N. Yamada. "Near-field radiative heat transfer between two parallel SiO<sub>2</sub> plates with and without microcavities." *Applied Physics Letters* 106.2 (2015): 023103.
- [12] Basu, Soumyadipta, Yue Yang, and Liping Wang. "Near-field radiative heat transfer between metamaterials coated with silicon carbide thin films." *Applied Physics Letters* 106.3 (2015): 033106.